Research Article

Cluster Synchronization in Networked Phase Oscillators under Periodic Coupling

S. S. Li [ID]

School of Mathematics and Information Science, North Minzu University, Wenchang North Street, Yinchuan 750021, Ningxia, China

Correspondence should be addressed to S. S. Li; sansanli@nmu.edu.cn

The synchronization behaviors of coupled oscillators under time-varying couplings are of both theoretical and practical significance. While recent studies show that synchronization is suppressed by time-varying coupling in general, the underlying mechanism is still not very clear. Here, by the kernel of sinusoidal coupling function, we revisit the effects of periodic coupling on the synchronization of networked phase oscillators. It is found that the suppressed synchronization by periodic coupling is attributed to the formation of synchronization clusters in the transition from desynchronization to global synchronization. The clusters are different in size and frequency but are all locked to the frequency of the periodic coupling. We demonstrate this phenomenon numerically in different network models and conduct a theoretical analysis on the numerical results based on the method of dimension reduction. The findings extend our knowledge on the dynamical responses of a complex network to external drivings, and shed lights on the mechanism of suppressed synchronization in periodically coupled oscillators.

1. Introduction

The study of collective behaviors covers many different fields, which range from physics to chemistry, biology, and social economy [1–4]. However, realistic systems are unavoidably affected by the surrounding circumstances. Typical examples include the seasonal variations in ecosystems [5], the circadian rhythm of the nervous system [6], the diurnal cycles on gene expressions [7], and the electrical and magnetic stimulations in brain areas [8]. Pharmacological and neurological evidence has revealed that the molecular and cellular pathology of neural disorders can be altered by externally added low-frequency periodic stimuli, yet the underlying mechanism remains unknown [8–10]. Revealing the mechanism behind these collective behaviors has always been an important research field of nonlinear dynamics and network science which expands the understanding of the macroscopic dynamics in complex systems [3, 4].

Synchronization is a typical collective behavior in network science. The Kuramoto model is a classical model to describe the synchronization phenomenon of coupled phase oscillators [1, 2]. When the coupling strength between oscillators exceeds a certain critical value (i.e., critical coupling strength K_c), the partial synchronization of coupled phase oscillators can be observed. As the coupling strength further increases, more and more oscillators are added to the synchronized cluster, forming a macroscopic nonzero order parameter. Since it was introduced, the classical Kuramoto model and its generalization have received wide attention aimed at analyzing collective synchronization [3, 4].

The robustness of synchronization to external perturbations is one of the central issues in probing oscillator synchronization. Due to the nonlinear characteristics of system dynamics, many interesting phenomena can be produced by the existence of external perturbations, e.g., the controlling synchronization by periodic signals [11–13], the steering synchronization by periodic drivings [14–18], the generating synchronization by specifying initial conditions [19], and the enhancing synchronization by random noise [20–23]. Similar studies also exist in ecosystems (where the interaction of biological species are changing with seasons) and metabolic systems (where gene expressions are affected

by diurnal cycles) [5, 7]. Recently, the field of time-varying coupling has received a great deal of attention [24–30]. It should be noted that periodic and even random modulation of the coupling strength does not always enhance synchronization [17, 31]. For example, periodic coupling suppresses synchronization in coupled phase oscillators in general, and the suppressed synchronization by periodic coupling has been attributed to the asymmetric oscillation of the temporal order parameter at the macroscopic scale [31]. However, it is still not very clear how this happened at the microscopic scale. In coupled nonlinear systems, some microscopical synchronous behaviors are exhibited when the inner elements compete or cooperate [29, 32]. In these studies, two questions are naturally raised: How the synchronization behaviors of coupled oscillators are affected by periodic couplings at the microscopic scale? How the critical coupling strength of coupled oscillators are affected by periodic couplings?

Motivated by the questions mentioned previously, we revisit how the synchronization behaviors of networked phase oscillators could be affected by periodic coupling [31]. Using the dimension reduction method, we analyze the impacts of periodic coupling on synchronization and give the formula of synchronization order parameter analytically. In particular, it is proven theoretically that the critical coupling strength remains unchanged by the periodic coupling. Numerical results demonstrate that the adoption of periodic coupling will suppress synchronization in general, showing the decreased synchronization order parameter as compared with the results of constant coupling. The theoretical predictions of the dimension reduction method are in good agreement with the results of numerical simulations. We investigate further the microscopic mechanism underlying the observed phenomena using the bifurcation tree, which shows clearly that the suppressed synchronization by periodic coupling is attributed to the formation of microscopic clustering patterns in the system. The findings shed lights on the interaction between complex nonlinear systems and external stimuli, and it might have implications for the interventions (evaluations) of function (operation) in some realistic systems, for example, the therapeutic interventions of neurological disorders, the control of cellular metabolism by diurnal cycles and circadian rhythm, and the evaluation of the impacts of seasonal variation on ecological processes [6–8].

The rest of this paper is organized as follows. In the next section, we will present the generalized model with a unimodal distribution of natural frequencies. In Section 3, we will derive a dimension reduction on the effects of periodic coupling on synchronization. Specially, we will provide rigorous proof of the critical strength coupling. In Section 4, we explore the microscopic mechanism of the suppressed synchronization, and discuss the generalizations to different network models, containing Zachary's karate club network and the neural network of nematode *C. elegans*. The conclusion will be given in Section 5.

2. The Generalized Model

We consider the dynamics of network-coupled phase oscillators governed by the following equations:

$$\dot{\theta}_i = \omega_i + \frac{K(t)}{d_i} \sum_{j=1}^{N} a_{ij} \sin\left(\theta_j - \theta_i\right), \tag{1}$$

with

$$K(t) = K_0[1 + \sin(\Omega t)], \tag{2}$$

where $i, j = 1, \ldots, N$ are the oscillator (node) indices, θ_i is the phase of the ith oscillator, and ω_i and N are, respectively, natural frequency of the ith oscillator and the size of the system. The natural frequency ω_i follows a prescribed probability density function $g(\omega)$. The coupling relationship between oscillators can be described by the adjacency matrix $\mathbf{A} = \{a_{ij}\}$, with $a_{ij} = a_{ji} = 1$ if two oscillators are connected by a link, otherwise $a_{ij} = a_{ji} = 0$. d_i represents the number of connections associated with oscillator i, that is, its degree. In contrast to the case of the classical Kuramoto model where the coupling strength among oscillators is an invariant constant, the generalized model considered here involves a coupling strength function $K(t)$ that depends on the coupling frequency Ω and coupling amplitude K_0 of periodic coupling [15]. If $\Omega = 0$, we have $K = K_0$ and the model is equivalent to the generalized Kuramoto model with constant coupling [4]. Furthermore, when all the oscillators are connected (i.e., $a_{ij} = a_{ji} = 1$ for all the nondiagonal elements in matrix $\mathbf{A}$), equation (1) depicts the classical Kuramoto model [4]. The main work of this paper is to investigate how the variations of Ω and K_0 will affect the synchronization degree of the oscillators at the microscopic scale.

Following the references [33, 34], we select the natural frequency ω_i from the Lorentzian distribution as follows:

$$g(\omega) = \frac{\Delta}{\pi} \frac{1}{\left(\omega - \omega_0\right)^2 + \Delta^2}. \tag{3}$$

Here, Δ and ω_0 are the scale parameter and the central frequency of the Lorentzian distribution, respectively. To describe the synchronization behaviors of the oscillator, Kuramoto introduces the macroscopic order parameter, which is defined as follows [2]:

$$z(t) = R(t)e^{\mathbf{i}\psi}$$

$$= \frac{1}{N} \sum_{j=1}^{N} e^{\mathbf{i}\theta_j}, \tag{4}$$

where $R(t)$ denotes the modulus of the complex order parameter $z(t)$, ψ is a collective phase, and $\mathbf{i} = \sqrt{-1}$ is an imaginary unit. $R \in [0, 1]$ describes the degree of synchronization between oscillators, such that $R = 0$ denotes the desynchronization state, whereas $R = 1$ is the global (perfectly) synchronization state.

3. Theoretical Analysis

To make the model theoretically tractable, we choose $N \longrightarrow \infty$ and employ the all-to-all coupling structure (all-coupled model). Using the dimension reduction method proposed by Ott and Antonsen [33, 34], we investigate the dynamical mechanism of the network-coupled phase oscillators. Under the thermodynamic limit condition ($N \longrightarrow \infty$), the state of the system at time t can be depicted by a continuous probability function $\rho(\theta, \omega, t)$. The evolution of $\rho(\theta, \omega, t)$ satisfies the continuity equation as follows:

$$\frac{\partial \rho(\theta, \omega, t)}{\partial t} + \frac{\partial [v_\theta \rho(\theta, \omega, t)]}{\partial \theta} = 0, \tag{5}$$

with

$$v_\theta(\theta, \omega, t) = \omega + \frac{K(t)}{2\mathbf{i}} \left[z(t)e^{-\mathbf{i}\theta} - z^*(t)e^{\mathbf{i}\theta} \right]. \tag{6}$$

The complex order parameter $z(t)$ is written in the continuous form as follows:

$$z(t) = \int_0^{2\pi} d\theta \int_{-\infty}^{+\infty} d\omega \, \rho(\theta, \omega, t)e^{\mathbf{i}\theta}. \tag{7}$$

Here, $z^*(t)$ denotes the complex conjugate of $z(t)$. Expanding the Fourier series of $\rho(\theta, \omega, t)$ with respect to θ, we can obtain the following:

$$\rho = \frac{g(\omega)}{2\pi} \left[1 + \sum_{n=1}^{\infty} \rho_n(\omega, t)e^{-\mathbf{i}n\theta} + c.c. \right]. \tag{8}$$

Here, $c.c.$ stands for the complex conjugate of $\sum_{n=1}^{\infty} \rho_n(\omega, t)e^{-\mathbf{i}n\theta}$. Using the Ott-Antonsen ansatz method [33, 34], we get

$$\rho_n(\omega, t) = [a(\omega, t)]^n, |a(\omega, t)| \leq 1, \tag{9}$$

we can obtain the following equations by substituting equation (8) into equations (5) and (7):

$$\frac{\partial a}{\partial t} + \mathbf{i}\omega a + \frac{K(t)}{2} \left[z(t)a^2 - z^*(t) \right] = 0, \tag{10}$$

$$z^*(t) = \int_{-\infty}^{\infty} d\omega a(\omega, t)g(\omega). \tag{11}$$

The Lorentzian distribution can be described as $g(\omega) = 1/(\mathbf{i}2\pi)[(\omega - \omega_0 - \mathbf{i}\Delta)^{-1} - (\omega - \omega_0 + \mathbf{i}\Delta)^{-1}]$. We thus obtain $z(t) = a^*(\omega_0 - \mathbf{i}\Delta, t)$ by the residue theorem. Substituting this result into equation (10), we obtain the following nonlinear equation with respect to the order parameter:

$$\frac{dR}{dt} + \left[\Delta - \frac{K(t)}{2} \right]R + \frac{K(t)}{2}R^3 = 0, \tag{12}$$

where R is the modulus of $z(t)$.

For the case of coupling frequency $\Omega = 0$, the solution of equation (12) is as follows [33, 34]:

$$R(t) = R_0 \left\{ 1 + \left(\frac{R_0^2}{R(0)^2} - 1 \right)e^{(2\Delta - K_0)t} \right\}^{-1/2}, \tag{13}$$

where $R_0 = \sqrt{1 - 2\Delta/K_0}$ and $R(0)$ is the initial value of the order parameter. Equation (13) shows that the value of R approaches R_0 for $K_0 > K_c = 2\Delta$ and approaches 0 for $K_0 < K_c$.

For the case of coupling frequency $\Omega \neq 0$, the desynchronization state is described by $R = 0$. The linearization of $R = 0$ is performed in equation (12). Letting $R = 0 + \delta R = \delta R$, we obtain

$$\frac{d\delta R}{dt} = \left[-\Delta + \frac{K(t)}{2} \right]\delta R - \frac{K(t)}{2}(\delta R)^3. \tag{14}$$

Neglecting the higher order term $o((\delta R)^2)$, we have

$$\frac{d\delta R}{dt} = \left[-\Delta + \frac{K(t)}{2} \right]\delta R. \tag{15}$$

Therefore, we get the averaged eigenvalue as follows:

$$\langle \lambda \rangle = \left\langle -\Delta + \frac{K(t)}{2} \right\rangle = -\Delta + \left\langle \frac{K(t)}{2} \right\rangle$$

$$= -\Delta + \frac{K_0}{2}. \tag{16}$$

Here, the brackets denote a time average. Hence, $R = 0$ will be transversely stable if $\langle \lambda \rangle < 0$. It is found that the frequency and amplitude of periodic coupling do not appear on the right-hand side of equation (16). This decoupling process shows that $\langle \lambda \rangle$ is the eigenvalue connected with the transverse perturbation δR (In the case where $R = 0$ is the incoherent state). If $\langle \lambda \rangle < 0$, we can deduce that $K_0 < 2\Delta$. Therefore, the critical coupling strength $K_c (= 2\Delta)$ is independent of periodic coupling, and it depends only on the scale parameter Δ of the Lorentzian distribution.

When $K_0 > K_c$, equation (12) cannot be solved analytically. Therefore, we use numerical simulation to solve it. By solving equation (12) numerically, the variation of R in the parameter space (Ω, K_0) is plotted in Figure 1. It shows that compared to the constant coupling, the synchronization performance of the system deteriorates with periodic coupling, and the order parameter R is gradually decreased with decreasing frequency of periodic coupling. Furthermore, equation (12) indicates that the evolution of R is independent of the central frequency, ω_0. These studies are in line with the findings in the periodically coupled phase oscillators [31]. Different from the previous study [31], we provide theoretical analysis for the critical strength coupling K_c that is independent of periodic coupling.

4. Numerical Results

In this section, we first consider the all-coupled case and show that suppressed synchronization emerges using periodic coupling. We verify our result using the theoretical analysis. Then, we explore the underlying microscopic
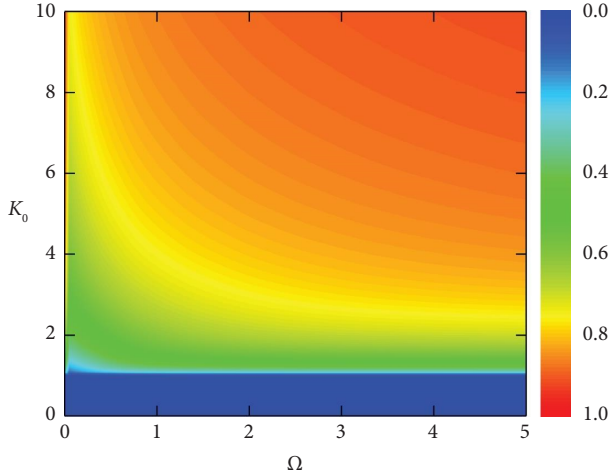
FIGURE 1: (Color online) for $\Delta = 0.5$ and $\omega_0 = 0$, the contour plot of R in the parameter space of (Ω, K_0) by solving equation (12). The color bar represents the magnitude of the order parameter, R.

mechanism based on the method of bifurcation tree, and finally, we extend the study to complex network cases.

4.1. All-Coupled Case. In numerical simulations, we choose the system size as $N = 10,000$, and update equations (1) and (2) using the fourth-order Runge–Kutta algorithm with step size $\delta t = 0.01$ and the transient time $T_{tr} = 200$. In obtaining the order parameter, R, we average the instant order parameter, $R(t)$, over a period of $T = 20$. Figure 2 (a1–c1) show the values of R versus the coupling amplitude K_0 in the all-coupled model. For all the cases, the values of R are staying around 0 when $K_0 < K_c \approx 1.0$. When $K_0 > K_c$, the value of R for the case of $\Omega = 2$ is clearly smaller than that of constant coupling ($\Omega = 0$), indicating that synchronization is suppressed. Furthermore, for the case of $\Omega = 9$, we find that the value of R is very close to that of constant coupling, signifying that synchronization is hardly affected. One can notice that the synchronization is suppressed for periodic coupling, and the theoretical results in equation (12) are in line with the simulation results in equation (1).

While recent studies show that synchronization is suppressed by time-varying coupling in general, the underlying mechanism is still not very clear [31]. Here, by the method of bifurcation tree, we illustrate the effects of periodic coupling on synchronization. To characterize the underlying mechanism, the microscopic effective frequencies are defined as follows [29, 32, 35]:

$$\langle \omega_i \rangle = \frac{1}{T_i} \int_t^{t+T_i} \dot{\theta}_i(t) \mathrm{d}t, \tag{17}$$

with T_i being the average time window. If two oscillators θ_i and θ_j are phase locked, then $\langle \omega_i \rangle = \langle \omega_j \rangle$, otherwise $\langle \omega_i \rangle \neq \langle \omega_j \rangle$. When all the oscillators have a common value, it implies that a global phase-locking of the system has occurred. However, if $\langle \omega_i \rangle$ behaves like a random form, it indicates that the system is in an incoherent state.

For the effective frequencies $\langle \omega_i \rangle$, we fix $t = 200$ and choose $T_i = 20$. Figure 2(a2–c2) plot the bifurcation trees of the effective frequencies $\langle \omega_i \rangle$ versus the coupling amplitude K_0 for different coupling frequencies $\Omega = 0, 2, 9$. It initially forms a cluster centered at the central frequency ω_0 for all three cases. For coupling frequency $\Omega = 0$, as coupling amplitude K_0 increases from 0, a majority of oscillators move close to $\langle \omega_i \rangle = 0$, and it finally generates a large cluster (Figure 2(a2)). For coupling frequency $\Omega = 2$, as coupling amplitude K_0 increases from 0, a majority of oscillators form several clusters which are centered at $k\Omega(k = \pm 1, \pm 2, \ldots)$ (Figure 2(b2)). This decreases the degree of synchronization and indicates that coupling frequency $\Omega = 2$ suppresses synchronization in coupled phase oscillators. As coupling amplitude K_0 continually increases, more oscillators merge into the synchronous cluster $\langle \omega_i \rangle = 0$. This phenomenon is different from the case of $\Omega = 0$. For coupling frequency $\Omega = 9$, as coupling amplitude K_0 increases from 0, a majority of oscillators form several clusters which are centered at $k\Omega(k = \pm 1, \pm 2, \ldots)$ (Figure 2(c2)). This decreases the degree of synchronization and indicates that coupling frequency $\Omega = 9$ suppresses synchronization in coupled phase oscillators. However, because $k\Omega(k = \pm 1, \pm 2, \ldots)$ are away from the central frequency ω_0, the degree of synchronization has hardly affected by the periodic coupling. It indicates that coupling frequency $\Omega = 9$ has little effect on the synchronization performance of coupled phase oscillators. As coupling amplitude K_0 continually increases, more oscillators merge into the synchronous cluster $\langle \omega_i \rangle = 0$. In contrast to the case of constant coupling ($\Omega = 0$), a majority of oscillators form several clusters which are centered at $k\Omega(k = \pm 1, \pm 2, \ldots)$ for $\Omega = 2, 9$. The clusters are different in size and frequency, but are all locked to the frequency of the periodic coupling (with a fairly uniform spacing between adjacent clusters). Furthermore, the closer is the central frequency ω_0, the bigger is the cluster size (Figure 2(a2–c2)).

Therefore, it is found that when coupling amplitude K_0 is small ($K_0 < K_c$), although the variation of Ω, the effective frequencies $\langle \omega_i \rangle$ are almost a random form for all the cases. As K_0 increases from K_c, the effective frequencies $\langle \omega_i \rangle$ have clearly several common values for the case of periodic coupling, indicating that synchronization is suppressed by periodic coupling. However, for the case of high-frequency coupling ($\Omega = 9$), we observe that the effective frequencies $\langle \omega_i \rangle$ are approximate to that of constant coupling for the whole area, signifying that synchronization is less influenced by high-frequency coupling. These studies demonstrate that the adoption of periodic coupling will suppress synchronization in general, and the degree of synchronization gradually deteriorates with decreasing the frequency of periodic coupling. The findings of this study are reported in the periodically coupled phase oscillators [31]. It is important to note that the suppressed synchronization is attributed to the formation of microscopic clustering patterns in our study, which was previously not found in the periodically coupled phase oscillators [31].
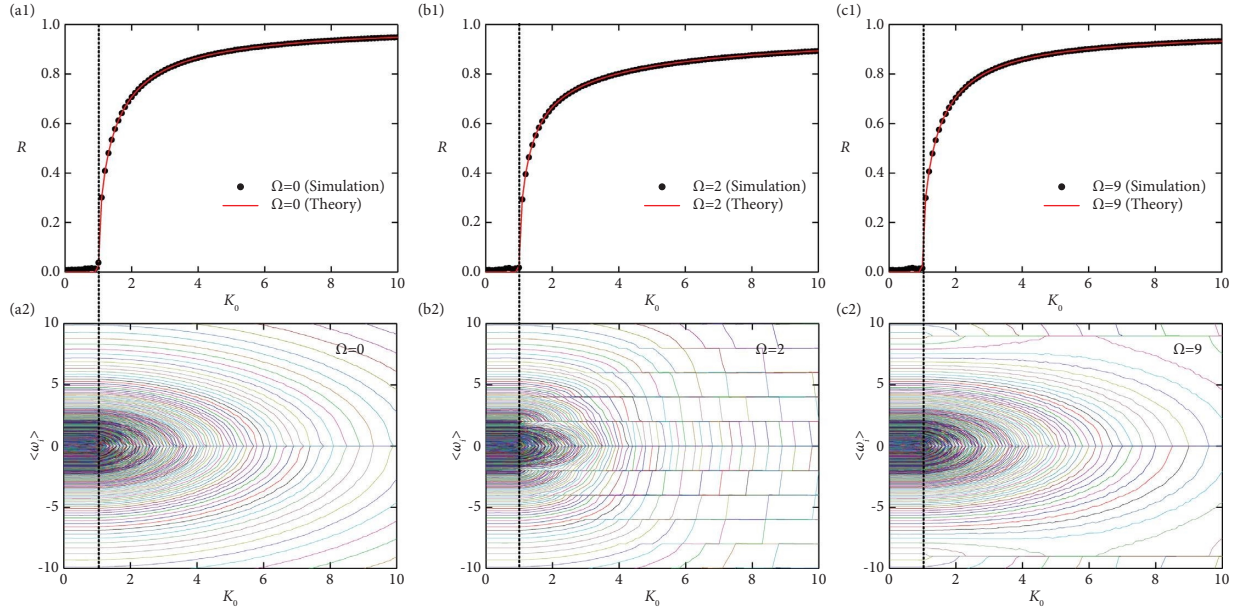
FIGURE 2: (Color online) the results for $\Delta = 0.5$ and $\omega_0 = 0$. (a1–c1) are the values of R versus the coupling amplitude, K_0 for different cases $\Omega = 0, 2, 9$, respectively. Black symbols and red lines, respectively, represent the numerical and theoretical results. (a2–c2) are, respectively, the bifurcation trees of $N = 10,000$ oscillators for different cases $\Omega = 0, 2, 9$, i e., the effective frequencies, $\langle \omega_i \rangle$, with respect to the coupling amplitude, K_0. The vertical dotted lines represent the critical coupling strength $K_c = 2\Delta$. For better display, the number of the oscillators is 1,000 evenly extracted from $N = 10,000$ of the simulations, and only the effective frequencies $\langle \omega_i \rangle$ in the range $[-10, 10]$ are displayed.

When the time scale of the nodal dynamics is almost identical to that of periodic coupling, the synchronization performance could be greatly changed in the periodically coupled chaotic oscillators [15]. In particular, it is shown that at some characteristic frequencies of the periodic coupling, the upper bound of stable synchronization in the parameter space of the coupling strength can be enhanced. For the periodically coupled phase oscillators, the averaged time scale of the nodal dynamics is measured by the central frequency ω_0 in the Lorentzian distribution. However, it is shown that ω_0 is irrelevant to the synchronization performance for periodic coupling [31]. This arouses our interest in studying the influence of ω_0 on synchronization using bifurcation trees.

Changing ω_0 to -2 and 2, we plot the variations of $\langle \omega_i \rangle$ with respect to K_0 for $\Omega = 2$ in Figure 3. We see that the clusters are different in size and frequency, but are all locked to $\omega_0 + k\Omega \, (k = \pm 1, \pm 2, \ldots)$. Furthermore, the closer is the central frequency ω_0, the bigger is the cluster size (Figures 2 and 3). This signifies that the clusters are dependent on the central frequency ω_0 and the frequency Ω of the periodic coupling. We also see that the results of $\omega_0 = -2$ and 2 are identical to that of $\omega_0 = 0$ except for the position of clusters. It suggests that the synchronization performance of periodically coupled phase oscillators is irrelevant to the time scale of the nodal dynamics (the central frequency ω_0 of the Lorentzian distribution). The results of this study are in line with the findings in the periodically coupled phase oscillators [31]. It should be noted that the main phenomenon is independent of the specific form of the frequency distribution. It has been verified from bifurcation trees that Gaussian distribution and the triangular frequency distribution also have similar phenomena.

4.2. Complex Network Cases. We finally test the universality of the observed phenomena in the system with complex network structures. The first system we investigate is the Zachary's karate club network which consists of 34 nodes and 78 links [36]. It is one of the most commonly used in complex networks, sociological analysis, and other fields. Significantly, it has two clusters in Zachary's karate club network. Besides the network structure, other settings of Zachary's karate club network are the same as the globally connected network in Figure 2, such as the coupling forms and the frequency distribution. Figure 4 shows the variations of $\langle \omega_i \rangle$ with respect to K_0 for the three cases of coupling frequency $\Omega = 0$, coupling frequency $\Omega = 0.3$ and coupling frequency $\Omega = 1$. We see that before the onset of synchronization, the effective frequencies of $\langle \omega_i \rangle$ for all three cases $(\Omega = 0, 0.3, 1)$ are very similar; after the onset point, the effective frequencies of $\langle \omega_i \rangle$ for the cases of $\Omega = 0.3, 1$ are different from that of constant coupling $(\Omega = 0)$. Specifically, we see that several clusters have been formed for $\Omega = 0.3, 1$. These results are in agreement with the results obtained in the globally connected network in Figure 2. It should be noted that due to the sparse connectivity of Zachary's karate club network, the synchronization order parameter is not precisely described by equation (12). However, we have revealed that the dynamic mechanism is universal, and is independent of the network structure (Figures 2 and 4). Therefore, we see that compared to the case of constant coupling, synchronization is suppressed by periodic couplings in general, and this is attributed to the formation of clusters. In addition, the spacing between adjacent clusters is identical to the frequency of periodic coupling.
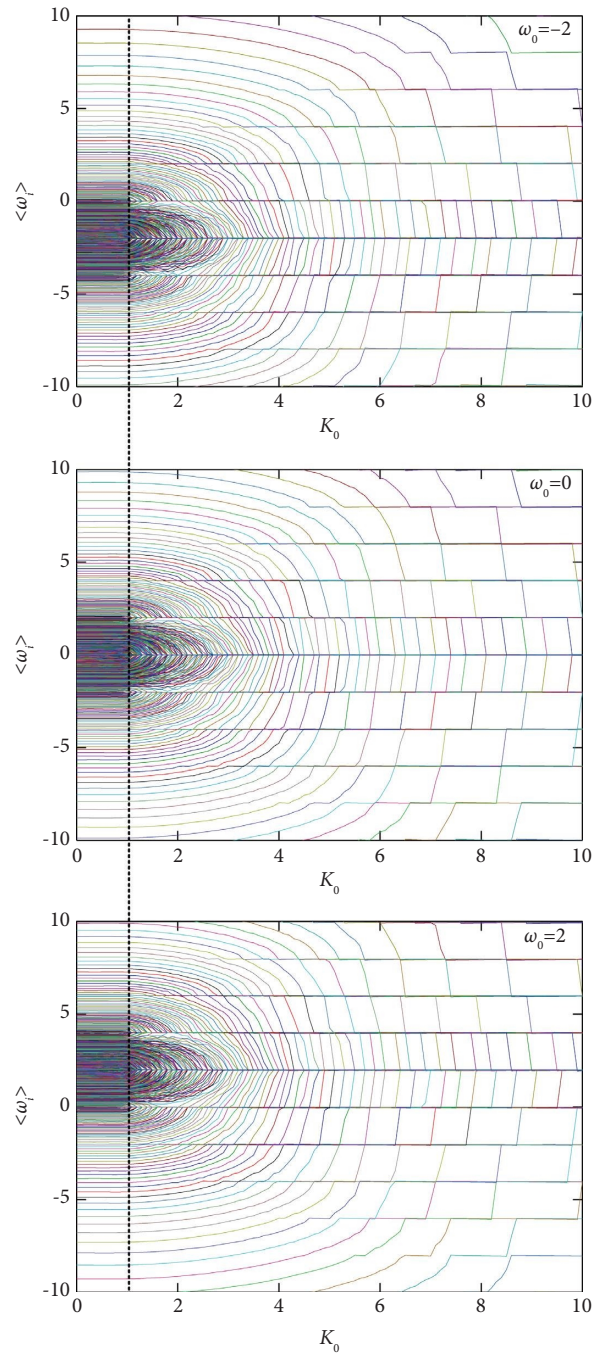
Figure 3: (Color online) for $\Delta = 0.5$ and $\Omega = 2$, the bifurcation trees of $N = 10,000$ oscillators for different cases $\omega_0 = -2, 0, 2$, i e., the effective frequencies, $\langle \omega_i \rangle$, versus the coupling amplitude, K_0. For better display, the number of the oscillators is 1,000 evenly extracted from $N = 10,000$ of the simulations, and only the effective frequencies $\langle \omega_i \rangle$ in the range $[-10, 10]$ are displayed. The vertical dotted line represents the critical coupling strength $K_c = 2\Delta$.
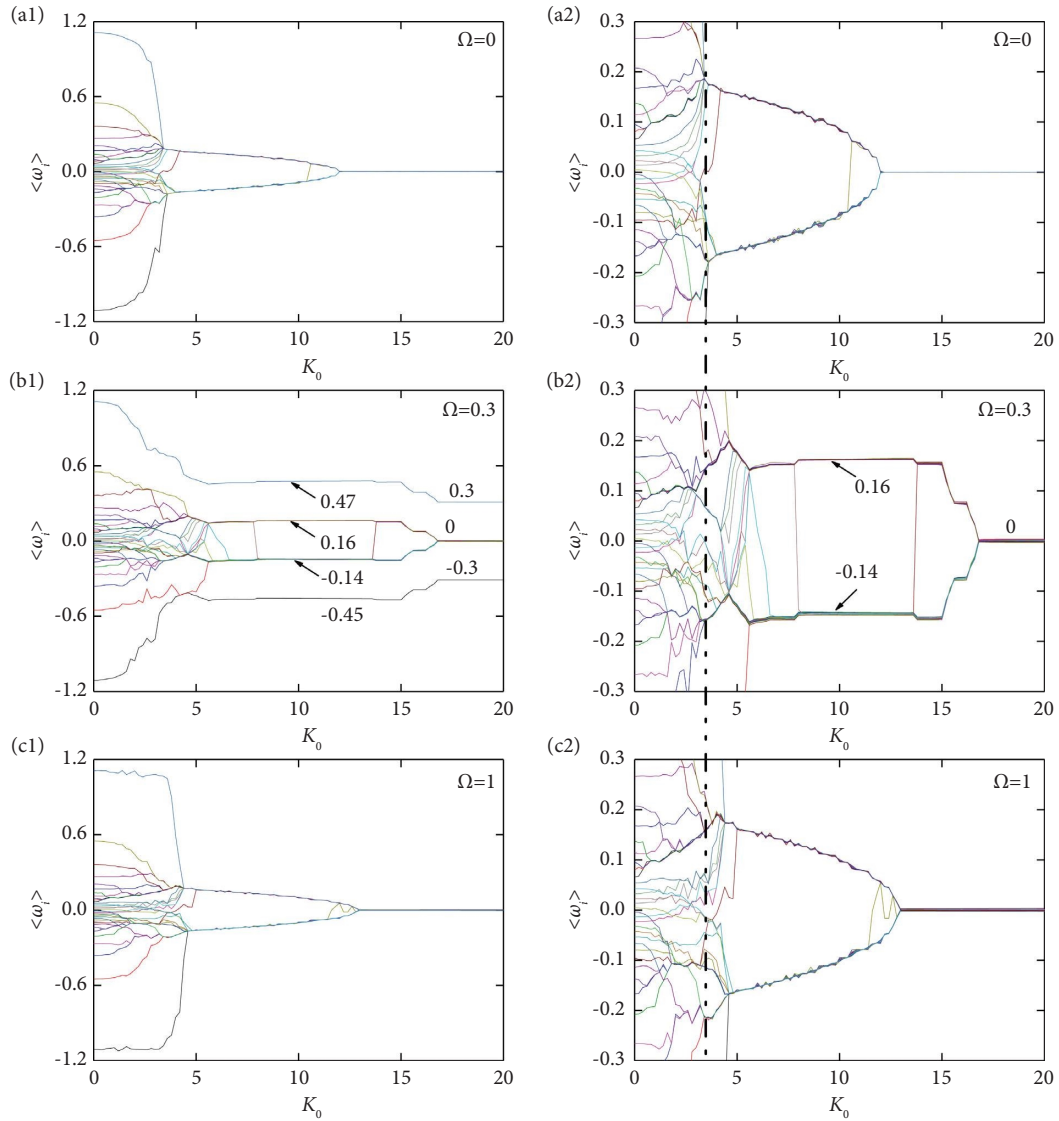
FIGURE 4: (Color online) for Zachary's karate club network of $\Delta = 0.1$ and $\omega_0 = 0$, the bifurcation trees of $N = 34$ oscillators for different cases $\Omega = 0, 0.3, 1$, i e., the effective frequencies, $\langle \omega_i \rangle$, with respect to the coupling amplitude, K_0. The left panel is the original image and the right panel is the enlarged image. The vertical dotted line represents the coupling strength $K_0 \approx 3.6$, which forms several clusters.

The second system we study is the neural network of the nematode *C. elegans*, which contains 297 nodes and 2,148 links [37]. The natural frequencies of the oscillators are still selected from the Lorentzian distribution, and the parameters are the same as those of the globally connected network (Figure 2). Figure 5 shows the variations of $\langle \omega_i \rangle$ with respect to K_0 for the cases of coupling frequency $\Omega = 0$, coupling frequency $\Omega = 1$, and coupling frequency $\Omega = 7$. The results are similar to the results of Zachary's karate club network (Figure 4), i.e., synchronization is suppressed by periodic couplings compared to the scenario of constant coupling. Therefore, periodic coupling suppresses synchronization in the general network structure and this is attributed to the formation of clusters.
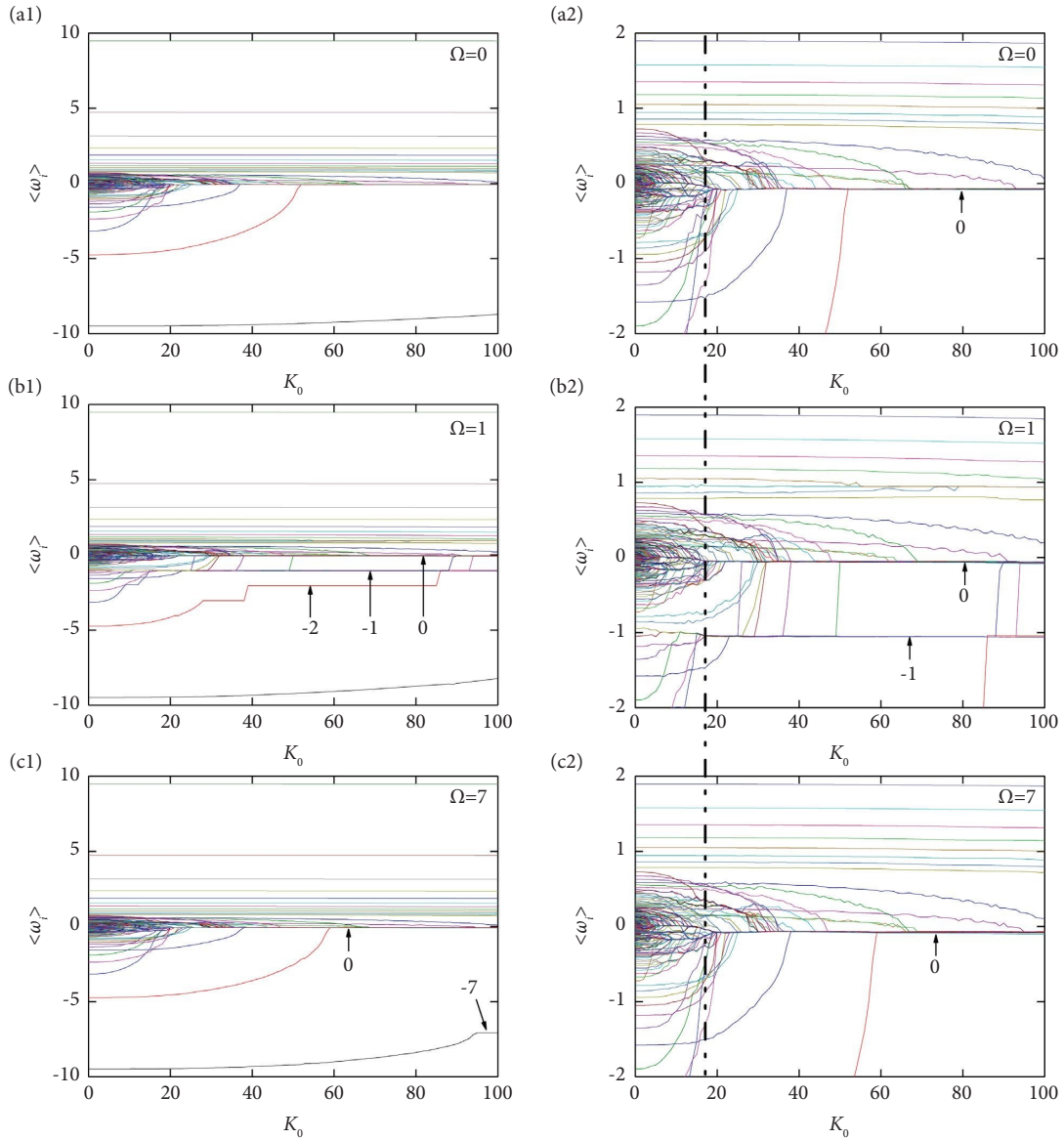
FIGURE 5: (Color online) for the neural network of the nematode *C. elegans* of $\Delta = 0.1$ and $\omega_0 = 0$, the bifurcation trees of $N = 297$ oscillators for different cases $\Omega = 0, 1, 7$, i e., the effective frequencies, $\langle \omega_i \rangle$, with respect to the coupling amplitude, K_0. The left panel is the original image and the right panel is the enlarged image. The vertical dotted line represents the coupling strength $K_0 \approx 17$, which forms several clusters.

5. Conclusion

As the dynamical basis of the normal brain function, the synchronous activity of distributed neurons has attracted the interest of neuroscientists [38]. In particular, there have been a variety of stimulation techniques aimed at improving the brain function or restoring the brain function from disorders in the past few decades [8, 9], including deep-brain stimulations and transcranial direct-current stimulations. Although this evidence has revealed that the molecular and cellular pathology of neural disorders can be changed by externally added low-frequency periodic stimuli. However, the underlying mechanism remains unclear.

The collective behavior of a complex system implies the emergence of a microscopic order from the organizations of populations of units with mutual interaction. Usually, the number of degrees of freedom at the macroscopic scale is so large that an exact description of the system at this level is impossible and also unnecessary. Therefore, a microscopic study of the complex system is significant [29, 32]. Here, treating the stimuli as periodic perturbations that modify the strength of couplings, we evaluate how the synchronization behaviors of networked phase oscillators could be affected by periodic coupling at the microscopic scale.

In summary, we have studied the generalized model with periodic coupling in which the coupling strength is changing periodically with time. We theoretically and numerically

verify that the critical coupling strength is irrelevant to the periodic coupling. The bifurcation trees have revealed that the system can exhibit rich clustering features in a system of finite size. The synchronization and desynchronization are characterized by the bifurcation tree, and the suppressed synchronization is attributed to the formation of clusters. In addition, these analyses can be generalized to realistic networks. The findings extend our knowledge on the dynamical responses of a complex network to external perturbations, and provide lights on the mechanism of suppressed synchronization in periodically coupled oscillators. Future studies could apply this model to study these periodically coupled biological, physical, social, and technological systems and to better understand their associated behaviors.

Data Availability

The data used to support the findings of this study are available upon request from the corresponding author.

Conflicts of Interest

The author declares that he has no conflicts of interest.

Acknowledgments

References

[1] A. Pikovsky, M. Rosenblum, and J. Kurths. Synchronization: a, *A Universal Concept in Nonlinear Sciences*, Cambridge University Press, Cambridge, UK, 2001.

[2] Y. Kuramoto, *Chemical Oscillations, Waves, and Turbulence*, Springer, Berlin, Germany, 1984.

[3] A. Arenas, A. Díaz-Guilera, J. Kurths, Y. Moreno, and C. Zhou, "Synchronization in complex networks," *Physics Reports*, vol. 469, no. 3, pp. 93–153, 2008.

[4] F. A. Rodrigues, T. K. D. Peron, P. Ji, and J. Kurths, "The Kuramoto model in complex networks," *Physics Reports*, vol. 610, pp. 1–98, 2016.

[5] M. Edwards and A. J. Richardson, "Impact of climate change on marine pelagic phenology and trophic mismatch," *Nature*, vol. 430, no. 7002, pp. 881–884, 2004.

[6] S. M. Reppert and D. R. Weaver, "Coordination of circadian timing in mammals," *Nature*, vol. 418, no. 6901, pp. 935–941, 2002.

[7] J. Stöckel, E. A. Welsh, M. Liberton, R. Kunnvakkam, R. Aurora, and H. B. Pakrasi, "Global transcriptomic analysis of Cyanothece 51142 reveals robust diurnal oscillation of central metabolic processes," *Proceedings of the National Academy of Sciences*, vol. 105, no. 16, pp. 6156–6161, 2008.

[8] H. Thomson, "How flashing lights and pink noise might banish Alzheimer's, improve memory and more," *Nature*, vol. 555, no. 7694, pp. 20–22, 2018.

[9] D. Fox, "Neuroscience: brain buzz," *Nature*, vol. 472, no. 7342, pp. 156–158, 2011.

[10] H. F. Iaccarino, A. C. Singer, A. J. Martorell et al., "Gamma frequency entrainment attenuates amyloid load and modifies microglia," *Nature*, vol. 540, no. 7632, pp. 230–235, 2016.

[11] V. Astakhov, A. Shabunin, and V. Anishchenko, "Synchronization of self-oscillations by parametric excitation," *International Journal of Bifurcation and Chaos*, vol. 8, no. 7, pp. 1605–1612, 1998.

[12] L. M. Childs and S. H. Strogatz, "Stability diagram for the forced Kuramoto model," *Chaos: An Interdisciplinary Journal of Nonlinear Science*, vol. 18, no. 4, Article ID 43128, 2008.

[13] J. Hindes and C. R. Myers, "Driven synchronization in random networks of oscillators," *Chaos: An Interdisciplinary Journal of Nonlinear Science*, vol. 25, no. 7, Article ID 73119, 2015.

[14] W. Yang, W. Lin, X. G. Wang, and L. Huang, "Synchronization of networked chaotic oscillators under external periodic driving," *Physical Review E*, vol. 91, no. 3, Article ID 32912, 2015.

[15] S. S. Li, N. Sun, L. Chen, and X. G. Wang, "Network synchronization with periodic coupling," *Physical Review E*, vol. 98, no. 1, Article ID 12304, 2018.

[16] J. S. Climaco and A. Saa, "Optimal global synchronization of partially forced Kuramoto oscillators," *Chaos: An Interdisciplinary Journal of Nonlinear Science*, vol. 29, no. 7, Article ID 73115, 2019.

[17] F. Baumann, I. M. Sokolov, and M. Tyloo, "Periodic coupling inhibits second-order consensus on networks," *Physical Review E*, vol. 102, no. 5, Article ID 52313, 2020.

[18] S. Yoon, E. A. P. Wright, J. F. F. Mendes, and A. V. Goltsev, "Impact of field heterogeneity on the dynamics of the forced Kuramoto model," *Physical Review E*, vol. 104, no. 2, Article ID 24313, 2021.

[19] V. Vinod, B. Balaram, M. D. Narayanan, and M. Sen, "Effect of configuration symmetry on synchronization in a Van der Pol ring with nonlocal interactions," *Nonlinear Dynamics*, vol. 89, no. 3, pp. 2103–2114, 2017.

[20] W. Lin and G. Chen, "Using white noise to enhance synchronization of coupled chaotic systems," *Chaos: An Interdisciplinary Journal of Nonlinear Science*, vol. 16, no. 1, Article ID 13134, 2006.

[21] K. H. Nagai and H. Kori, "Noise-induced synchronization of a large population of globally coupled nonidentical oscillators," *Physical Review E*, vol. 81, no. 6, Article ID 65202, 2010.

[22] Y. M. Lai and M. A. Porter, "Noise-induced synchronization, desynchronization, and clustering in globally coupled nonidentical oscillators," *Physical Review E*, vol. 88, no. 1, Article ID 12905, 2013.

[23] D. Frydel, "Kuramoto model with run-and-tumble dynamics," *Physical Review E*, vol. 104, no. 2, Article ID 24203, 2021.

[24] E. V. Rybalova, T. E. Vadivasova, G. I. Strelkova, and A. Zakharova, "Multiplexing noise induces synchronization in multilayer networks," *Chaos, Solitons & Fractals*, vol. 163, Article ID 112521, 2022.

[25] D. Ghosh, M. Frasca, A. Rizzo et al., "The synchronized dynamics of time-varying networks," *Physics Reports*, vol. 949, pp. 1–63, 2022.

[26] S. B. Zhu, J. Zhou, X. H. Yu, and J. A. Lu, "Synchronization of complex networks with nondifferentiable time-varying

delay," *IEEE Transactions on Cybernetics*, vol. 52, no. 5, pp. 3342–3348, 2022.

[27] Q. Jia, Z. Y. Han, and W. K. S. Tang, "Synchronization of dynamical networks with heterogeneous delays via time-varying pinning," *IEEE Transactions on Circuits and Systems I: Regular Papers*, vol. 69, no. 9, pp. 3783–3793, 2022.

[28] Y. G. Wu, Z. G. Zheng, L. K. Tang, and C. Xu, "Synchronization dynamics of phase oscillator populations with generalized heterogeneous coupling," *Chaos, Solitons & Fractals*, vol. 164, Article ID 112680, 2022.

[29] Z. K. Cai, Z. G. Zheng, and C. Xu, "Exact dynamics of phase transitions in oscillator populations with nonlinear coupling," *Communications in Nonlinear Science and Numerical Simulation*, vol. 107, Article ID 106129, 2022.

[30] X. D. Liu, "Heterogeneous phase oscillators under symmetry breaking of coupling strength: optimal synchronization and desynchronization under strong gain," *Physica A: Statistical Mechanics and Its Applications*, vol. 606, Article ID 128093, 2022.

[31] S. S. Li, X. G. Wang, and S. G. Guan, "Periodic coupling suppresses synchronization in coupled phase oscillators," *New Journal of Physics*, vol. 20, no. 11, Article ID 113013, 2018.

[32] X. Huang, J. Dong, W. J. Jia, Z. G. Zheng, and C. Xu, "Dynamics of clustering patterns in the Kuramoto model with unidirectional coupling," *Frontiers of Physics*, vol. 13, no. 5, Article ID 130506, 2018.

[33] E. Ott and T. M. Antonsen, "Low dimensional behavior of large systems of globally coupled oscillators," *Chaos: An Interdisciplinary Journal of Nonlinear Science*, vol. 18, no. 3, Article ID 37113, 2008.

[34] E. Ott and T. M. Antonsen, "Long time evolution of phase oscillator systems," *Chaos: An Interdisciplinary Journal of Nonlinear Science*, vol. 19, no. 2, Article ID 23117, 2009.

[35] Z. G. Zheng, G. Hu, and B. B. Hu, "Phase slips and phase synchronization of coupled oscillators," *Physical Review Letters*, vol. 81, no. 24, pp. 5318–5321, 1998.

[36] W. W. Zachary, "An information flow model for conflict and fission in small groups," *Journal of Anthropological Research*, vol. 33, no. 4, pp. 452–473, 1977.

[37] J. G. White, E. Southgate, J. N. Thompson, and S. Brenner, "The structure of the nervous system of the nematode *C. elegans*," *Philosophical Transactions of the Royal Society of London*, vol. 314, pp. 1–340, 1986.

[38] F. Varela, J. P. Lachaux, E. Rodriguez, and J. Martinerie, "The brainweb: phase synchronization and large-scale integration," *Nature Reviews Neuroscience*, vol. 2, no. 4, pp. 229–239, 2001.